20259054

Comparative studies on the performance of Antilock Braking System for a hybrid brake-by-wire system in EV application

Marius Heydrich Valentin Ivanov

Thuringian Center of Innovation in Mobility, Smart Vehicle Systems, Ilmenau, Germany

E-mail: marius.heydrich@tu-ilmenau.de

ABSTRACT: This paper presents a case study on the performance of antilock braking system, especially tailored for use in electric vehicles with brake-by-wire system. In particular, a hybrid system layout with both, electrohydraulic and electromechanical brakes is discussed. Hence, the proposed controller and the control gains are adjusted accordingly to the different system dynamics. Within hardware-in-the-loop experiments on the real braking system, remarkable improvements about active safety and control robustness were achieved and evidenced through the assessment of objective performance indicators.

KEY WORDS: antilock braking system, brake-by-wire, electrohydraulic brakes, electromechanical brakes

1. INTRODUCTION

Humans have an inherent desire for mobility and flexibility. Foreseeable, that the number of vehicle first registrations in 2023 increased by +14 % (~12.8 million units) in Europe, +12 % (~15.5 million units) in the United States, and +5 % (~21.7 million units) in Asia in comparison to 2022.[1] However, with more vehicles on the road, also the number of accidents may rise, but the amount of lethal endings decreases constantly. This is due to more and more active safety systems in modern vehicles.

One of the best-known and also one of the oldest ones is the antilock braking system (ABS). Through the modulation of brake torque, it prevents the wheels from locking at aggressive braking manoeuvers to maintain optimal force transmission between tire and the underground. The first ABS was already invented in the late 1970s, and took its stand as one of the most relevant active safety systems through the years. Hence, it is natural, that there is still research in progress, especially on new methods of controlling the wheel slip between tire and underground.

In the past, mostly rule-based (RB) methods[2] were used for controlling the wheel slip, due to their robust operation and low computational power. Anyway, these controllers waste potential and need excessive tuning on the target platform[3]. With the upcoming trend for microcomputers instead of microcontrollers and the larger computational power, new methods were enabled for integration. Especially continuous control approaches received more and more attraction, such as proportional-integral (PI)[4],[5], model-predictive[6],[7], fuzzy[8]-[11] and sliding mode[5],[12]-[14] controls shall be named here.

Besides the higher computational power of the control units, the introduction of decoupled brake systems on the market accelerated development of continuous control approaches too. Especially electromechanical brakes (EMBs) will need adaptive algorithms to exploit their full potential for vehicle dynamics control, but by today, they have not reached maturity yet. Therefore, the previously mentioned studies still concentrate either on passive brakes[10],[11], simulations[12],[13] or experiments with electrohydraulic brakes (EHBs)[5]-[7],[9], since latter ones have reached market readiness and are already in use. Moreover, their already higher dynamics making them a good candidate for testing continuous approaches at system level. However, they still do have many disadvantages of hydraulic brakes, since they feature most of the conventional parts, limiting their performance. Thus, hybrid brake-by-wire layouts are a reasonable alternative, since they combine EHBs and EMBs to use as many benefits of both. There are already systems available, that use one brake circuit with EHBs for the front and EMBs for the rear axle, making them compliant with technical regulation[15],[16].

In the present research, a case study on ABS with regard to gain tuning for optimal performance evaluation is presented. In particular, it continues former work[17] conducted on a hybrid brake-by-wire system for use in electric vehicles. The article is structured as follows: The next section will summarize the research problem as well as methodology of the experiments. Right after, the analysis of the results is carried out, before the achievements are summarized in the conclusion.

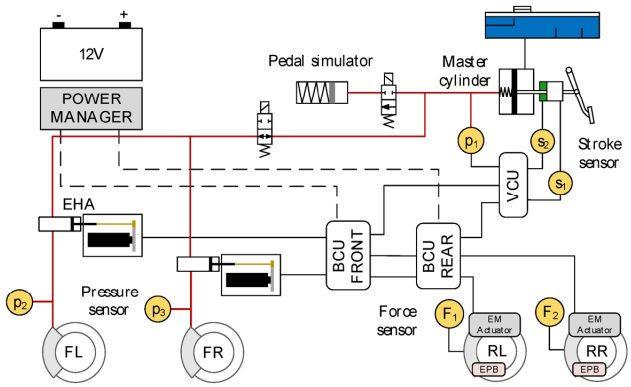

Fig. 1 Scheme of the hybrid brake-by-wire system[18]

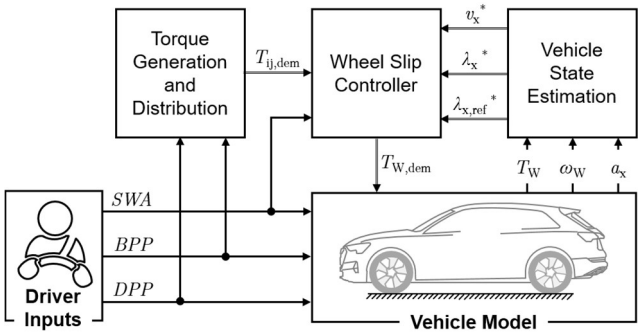

Fig. 2 Scheme of the integrated controller structure

3. Research Demand and Methodology

Aforementioned, hybrid architectures are already in use and a promising alternative to pure (electro)hydraulic brake systems on the market. Therefore, the research is conducted on a hybrid brake-by-wire system for an electric vehicle (see Fig. 1) for evaluation of ABS performance.

The used vehicle control is shown in Fig. 2 and consists of three main part. The block "torque generation and distribution" uses the drive (*DPP*) and brake pedal position (*BPP*) to calculate the torque demand for every wheel ($T_{ij,dem}$), where the index i (i = F, R) stands for the axle and j for the side (j = L, R), respectively. The ABS is part of the block "wheel slip controller", which also receives the steering wheel angle (*SWA*) as an input, since the control gets inactive by reaching a specific level of lateral dynamics. Main target of ABS control is to prevent the wheels from locking by maintaining a specific wheel slip during braking. The slip at every wheel corner can be calculated with the wheel speed (ω_w), dynamic wheel radius (r_w) and the longitudinal velocity (v_x^*) as shown below, where * marks estimated parameters.

$$\lambda_x^* = -\frac{v_x^* - \omega_w r_w}{\max(v_x^*, \omega_w r_w)} \tag{1}$$

For ABS control in the current study, a proportional-integral (PI) controller is investigated, since it is widely used in industrial applications. The commonly used derivative part, that is used to prevent the controller from overshooting, is replaced by an anti-windup part, since derivative gains are very sensitive to noise in the measurement. The control law is given in eq. (2), where K_P is the proportional gain, t_i and t_a is the time constant of integral and anti-windup part, respectively, and τ is the integration step. The input is the slip error $\lambda_e = \lambda_{ref}^* - \lambda_x^*$ with the reference slip λ_{ref}.

$$u_{PI} = K_p \left(\lambda_e + \int_{t=0}^{\tau} \frac{\lambda_e}{t_i} - t_a \, \mathrm{sat}(u_{PI}) \, \mathrm{d}t \right) \tag{2}$$

Further, an integral-sliding mode (ISM) controller is used for comparison with standard PI. The corresponding control law is given by eq. (3), where K_{ISM} is the control gain and s is the sliding surface, that was described in former publications[5],[18].

$$u_{ISM} = u_{PI} - K_{ISM} \, \mathrm{sign}(s) \tag{3}$$

Previous experiments on the system[18] proved, that the EHBs and EMB do obviously have different dynamics. Hence, an equal tuning for both axles is not feasible. This article investigates an axle-wise gain tuning (see Table 2 in the appendix), tailored to the system dynamics. The setting is tested in several straight-line-braking manoeuvers with five different conditions in total:

- ***High μ*** relates to homogenous adhesion of $\mu = 0.9$.
- ***Low μ*** relates to homogenous adhesion of $\mu = 0.4$.
- ***Split μ*** relates to high μ condition on one and low μ condition on the other vehicle side.
- ***Longitudinal split μ*** relates to a step from high μ to low μ condition across the driving direction.
- ***Patch μ*** is designed with a pattern of different adhesion coefficients along the way (see Fig. 3). This can be the case e.g., in fall, when there are puddles with different water level or wet leaves on the road.

Latter manoeuver is used for robustness assessment, since the control must adapt itself to the varying circumstances. For both of the latter manoeuvers, vehicle stability is a crucial point, since the different adhesion on both side, may lead the vehicle to yaw.

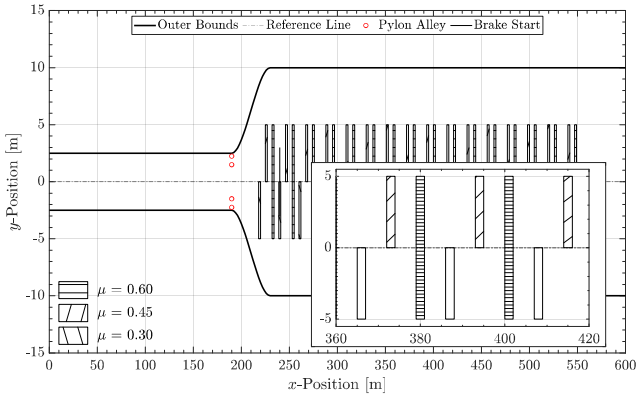

Fig. 3 Scenario setup for patch-μ manoeuver

Table 1 Target electric vehicle model data

Parameter	Symbol	Unit	Value
Vehicle total mass	m_v	[kg]	2715
Driveline topology	-	-	RWD
Motor layout	-	-	in-wheel
Motor type	-	-	PMSM
Max. motor torque	$T_{em,max}$	[Nm]	1500
Max. motor power	$P_{em,max}$	[kW]	110
Front Brakes			
Disc size	$D_{fb,f}$	[mm]	375
max. brake torque	$T_{fb,f}$	[Nm]	4000
Front Brakes			
Disc size	$D_{fb,r}$	[mm]	350
max. brake torque	$T_{fb,r}$	[Nm]	1600
Tire size	-	-	255/50 R20
Dynamic tire radius	r_{dyn}	[mm]	378

To investigate the performance in a broad range, every road condition was simulated at different initial vehicle speeds, which are referring to speed limits in different traffic scenarios. In summary, the data contains five road conditions, five initial speeds, three control strategies with five repetitions per setup, making a total of 375 simulations. As stated in the Introduction already, the experiments are similar to previous the authors' previous work [17]. Hence, the same vehicle model is used, see Table 1. For higher reliability of the results, a hardware-in-the-loop test bench is used, featuring the brake-by-wire system from Fig. 1, a power supply, experimental harness and a real-time processing unit from company dSPACE as it was outlined in former work.[17] This ensures, that the system dynamics are considered in the tests, but thermal effects are neglected. To evaluate the control performance in an adequate and reliable way, some objective indicators are defined as follows.

First indicator is the medium deceleration (d_m) as a direct measure for the efficacy of force transmission between the tires and road. In the ECE regulation No. 13H[19], the deceleration is calculated according to eq. (4), where v_{80} and v_{10} are the velocities (in [km/h]) that equal 80 % and 10 % of the initial vehicle speed and s_{80} and s_{10} (in [m]) are the corresponding distance values. This ensures, that the application dynamics and slip identification artifacts are excluded, because only the "linear" part is evaluated.

$$d_m = \frac{{v_{80}}^2 - {v_{10}}^2}{25.92\,(s_{10} - s_{80})} = \frac{{v_{init}}^2}{0.0243\,(s_{10} - s_{80})} \tag{4}$$

However, the limits seem unsuitable for e.g., brake distance (s_{br}), since it gets normally evaluated between the time, when the brake action is initiated until vehicle standstill. In the studies, this is the case, as soon as the brake pedal position (BPP) exceeds 5 % ($t_{br,0}$) and the vehicle speed falls under 0.1 km/h ($t_{br,1}$). The braking distance is a direct metric for active safety.

$$s_{br} = \int_{\tau = t_{br,0}}^{t_{br,1}} v\,\mathrm{d}\tau = s(t_{br,1}) - s(t_{br,0}) \tag{4}$$

Another important metric is the controller's ability to track the reference wheel slip, so the *root mean square tracking error* (*TE*) is evaluated next. It is evaluated for the front left (FL) and rear right (RR) wheel in the studies.

$$TE(ij) = \sqrt{\frac{1}{N}\sum_{k=1}^{N}\left({\lambda_{x,ref}}^* - {\lambda_x}^*\right)^2} \tag{5}$$

The *integral of absolute control action* sums up the changes in the brake torque (ΔT) due to the torque modulation control of ABS during the manoeuver. This KPI was introduced by Tavernini et al.[7] and represents stress on the brake system and brake wear.

$$IACA = \frac{1}{t_{br,1} - t_{br,0}} \int_{\tau = t_{br,0}}^{t_{br,1}} |\Delta T| \mathrm{d}\tau \tag{6}$$

Beside longitudinal dynamics, braking under inhomogeneous conditions will lead to yaw motion too. Especially for untrained or unexperienced drivers, a steep increase and/or change of the yaw rate can be crucial to handle. Therefore, the ABS is normally combined with a stability control. In this study, no stability control is implemented, but the driver (model) is given freedom to react on deviations from the reference trajectory e.g. by steering to the opposite direction. By evaluating the *peak-to-peak yaw rate value*, an indicator is given, how much lateral dynamics occurred during the manouevers.

$$\dot{\Psi}_{p2p} = \max(\dot{\Psi}) - \min(\dot{\Psi}) \tag{7}$$

4. Results and Discussion

In the following sections, the relevant test data is evaluated to assess the behavior of the controller through quantification of the key performance indicators (KPIs) from eq. (4)-(7). In Fig. 4 all results are given graphically, where the white bars indicate the maximum of all considered simulations, while the colored ones indicate the minimum, respectively. The improvements against the reference scenario (RB) are given in Table 3-7 in the appendix, where positive values indicate improvements, while negative ones indicate performance loss. The yaw rate is not included in Table 2 due to the observations in the test data, that will be explained in the next paragraphs.

(a) *Manoeuvers on high μ surface*

As stated previously[17], the results on high μ do not show significant variance in the data of all controllers under investigation. Foreseeable, brake distance and mean deceleration increase with higher initial speeds. As given by eq. (4), the value is determined between v_{80} and v_{20}, so with higher initial speeds, this range becomes bigger and more samples at higher values are considered, shifting the mean value. In particular, braking distance and mean deceleration at lower initial speeds showed no remarkable improvements in all cases (see Table 3), so the focus lies on the other results. Anyway, some further outcome is observable. Due to the high adhesion of the surface, much higher braking forces are transmittable before wheel lock, so the values for the mean deceleration are the highest among all test setups. Further, the continuous approaches (ISM, PI) are able to increase the values up to 100 km/h. At higher speeds, the differences are nearly equalized, see Fig. 4, since ISM and PI control are able to stay below the minimum tracking error value of the RB control. For the IACA, the values increase slightly to improve slip tracking.

(b) *Manoeuvers on low μ surface*

More relevant are the results at low adhesion potential. For 130 km/h, the mean deceleration increased by 26 % and brake distance decreased by 13.5 % in comparison with the RB control, which equals up to 26 m. With a deep look, it gets clear, that the RB control lacks in tracking the reference slip with an error of over 80 % (FL), while ISM and PI just show half the value. More interesting is the performance on the RR wheel.

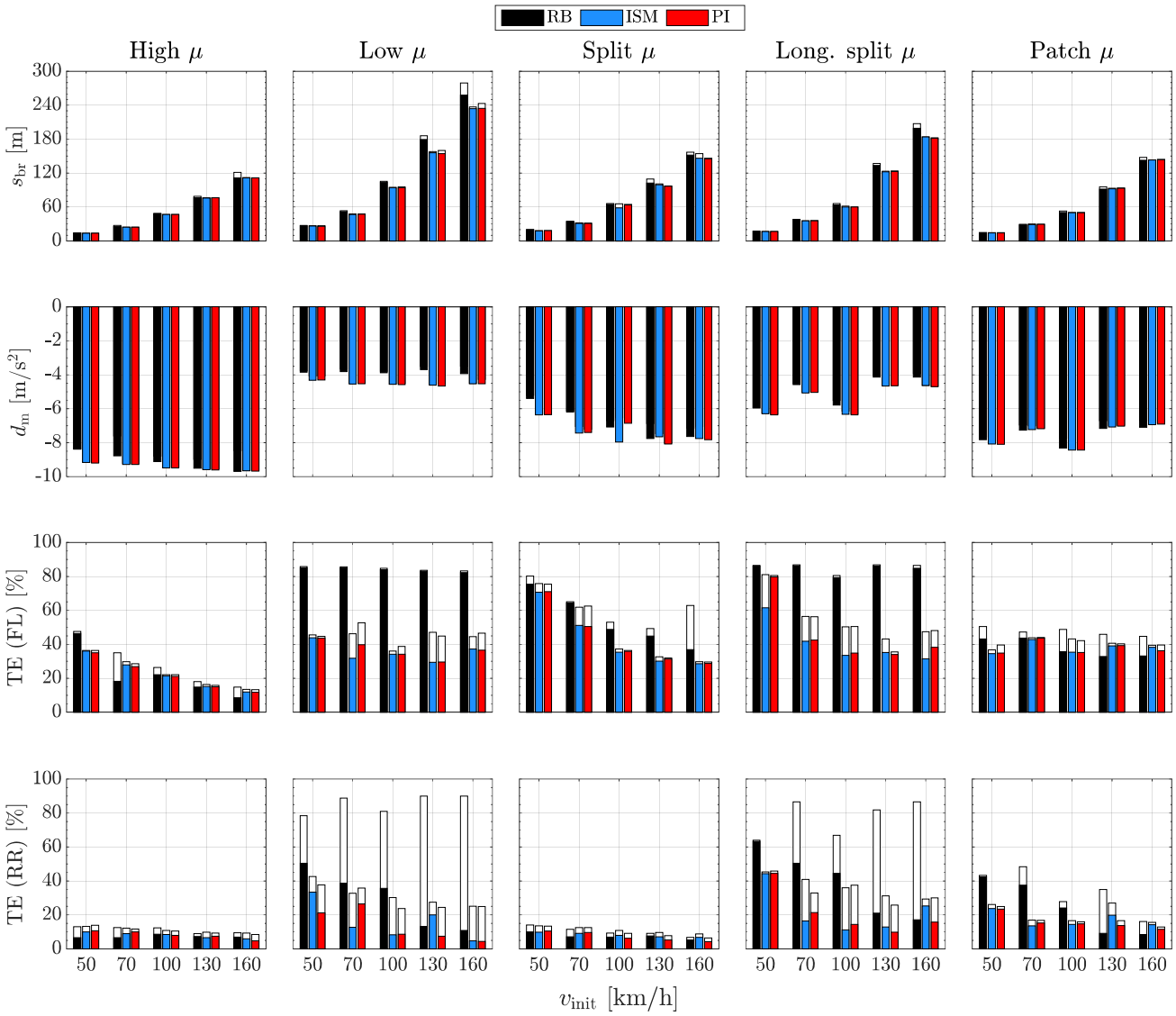

Fig. 4 Experimental results and primary KPI assessment for all straight-line braking manoeuvers.

The mean tracking error lies between 45.3 % and 64.5 % (RB), and between 18.6 % and 22.6 % (ISM) as well as 14.7 % and 25.9 % (PI), see Table 4. These are improvements of up to 70 %, showing the superior performance of the continuous approaches in combination with the fast dynamics of EMBs under severe conditions. Especially on wet or icy road, the improvement towards higher deceleration values is important to prevent hazardous situations. In fact, the IACA was decreased by over 23% in all simulations for PI and ISM compared to the RB approach, related to the better tracking performance. Since the slip error is kept lower from the beginning, the change of the overall control demand appears less frequently.

(c) *Manoeuvers on split μ surface*

While the previous scenarios were targeting the assessment of active safety, the next one deals with the vehicle stability as any brake event can lead to severe harm, if the vehicle starts spinning as a results of lateral stability loss. Therefore, the scenario with inhomogeneous road surfaces is used to evaluate the performance. In this particular case, KPIs such as brake distance or mean deceleration step in the background. Figure 5 depicts the results. The rule-based control performed better with regard to the peak-to-peak yaw rate. Having a closer look on the wheel slip tracking, no remarkable differences can be seen, so further experiments with particular regard to these abnormalities must be conducted in future. Besides the peak-to-peak of the yaw rate, eq. (7) is used for the pitch rate. Neglecting characteristics of the suspension system, the pitch rate can be used to justify other data or to check plausibility. Referring to general brake dynamics and the rubber friction theory by Kummer[20], the wheel loads change as soon as an external force acts on the vehicle, which increase force transmission potential. For the braking, this means that the rear axle lifts, while the front axle gains additional load. The faster, the deceleration is built up, the higher the pitch rate.

(d) *Manoeuvers on longitudinal split μ surface*

A similar behavior can be observed for the longitudinal split manoeuver, where the brake distance was decreased by 10-13 %. One exception is the scenario at 50 km/h initial speed. There is one curiosity, since the mean deceleration is clearly higher for 50 km/h and 100 km/h initial vehicle speed, what is related to one setup for low speeds (< 100 km/h) and high speeds (≥ 100 km/h) as well.

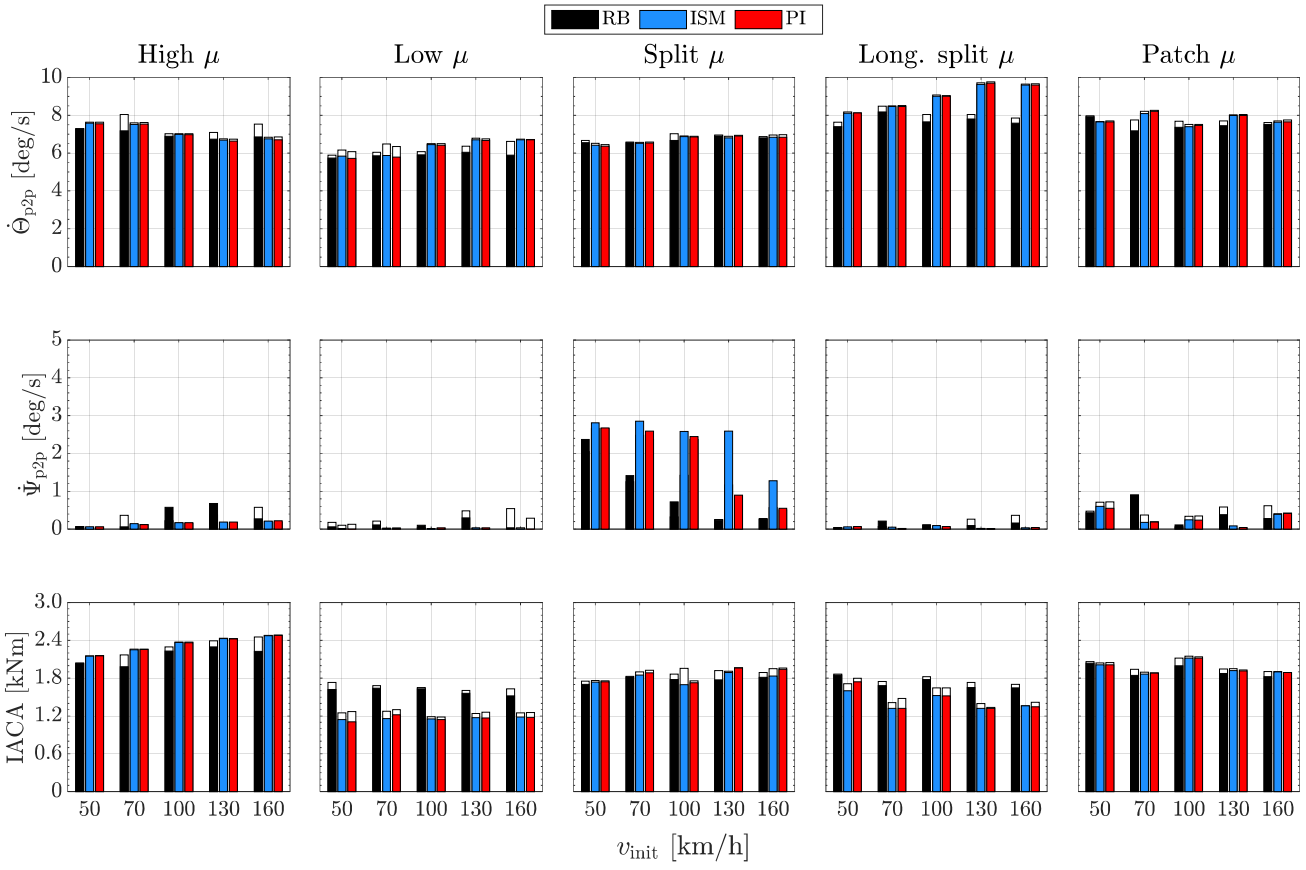

Fig. 5 Experimental results and secondary KPI assessment for all straight-line braking manoeuvers.

Both differ in the length of the high μ section. Obviously, the faster the vehicle enters the manoeuver, the earlier it reaches the μ step. This leads to a longer period on the low adhesion surface and therefore to a lower mean deceleration. A second reason is the evaluation with eq. (4), since it assumes the deceleration curve to be linear, but its slope varies after passing the step. Therefore, this KPI should be treated with cautiousness for this manoeuver. Even though, the absolute peak-to-peak yaw rate appears to be quite small, but it is hard to define borders, since every driver reacts differently to yaw dynamics. As a reference, the research of Zhang et al.[21] is used, showing that a lane change on the highway performed by different driver types lead to a peak-to-peak yaw rate values of less than 8 deg/s (normal driver) or 5 deg/s (cautious driver), respectively. Applied to the current results, the yaw rate is not critical, so even a cautious driver can stabilize the vehicle at minimal effort. In can be observed, that the peak-to-peak pitch rate is higher in all these manoeuvers in general and for the continuous approaches in particular. This occurs, when the vehicle enters the low adhesion surface with the braking forces from previous high adhesion region, leading to an additional impulse. This widens the range and leads to higher peak-to-peak values.

(e) *Manoeuvers on patch μ surface*

The last manoeuver is performed with a very inhomogeneous surface, which is perfect for testing both, vehicle stability and controller robustness, respectively. The results show, that the overall performance is similar to the longitudinal split scenario, but it must be stated, that the continuous controls lack superiority. Only the wheel slip tracking on the rear axle shows better results against the rule-based method, which leads to slightly smaller brake distances. However, the differences are not remarkably high. Considering the yaw and pitch dynamics, no negative effects can be seen. The peak-to-peak pitch rate ratio behaves as expected and the yaw rate do not raise over the values for the high μ manoeuver, so no instable vehicle state will occur.

4. CONCLUSIONS

The present article introduced a case study on the gain tuning of antilock braking system particularly used with a hybrid brake-by-wire system. In particular, a proportional-integral as well as an integral sliding mode control approach were benchmarked against a classical rule-based ABS. The effect(s) on the brake performance were experimentally investigated via hardware-in-the-loop tests on the real actuators and measured through dedicated KPIs. The results showed superiority of the continuous approaches against the rule-based one, showing better slip tracking and therefore minimizing braking distance in all manoeuvers. Especially under severe conditions (e.g., braking on low adhesion or with spontaneous adhesion decrease), the new controllers improved active safety significantly while maintaining sufficient vehicle stability. To verify robustness of the control for different scenarios, several tests with inhomogeneous road conditions were conducted. Again, the results were promising and verified the performance improvement. In future research the results should be validated through in-vehicle testing.

ACKNOWLEDGMENT

The research leading to these results was funded by the European Union under the Horizon 2020 and Horizon Europe Research and Innovation Programmes under Grant Agreement No. 824250 (EVC1000) and No. 101056824 (HighScape). Views and opinions expressed are however those of the author(s) only and do not necessarily reflect those of the European Union or the European Climate, Infrastructure and Environment Executive Agency (CINEA). Neither the European Union nor CINEA can be held responsible for them.

REFERENCES

(1) J. Cholewa, “Pkw International,” German Association of the Automotive Industry (VDA), [Online]. Available: https://www.vda.de/de/themen/automobilindustrie/neuzulassungen-pkw-und-e-pkw/international (accessed: October 21, 2024)

(2) K. Reif (Ed.), “*Brakes, Brake Control and Driver Assistance Systems. Funtion, Regulation and Components*,” Springer Vieweg, 2014

(3) F. Pretagostini et al., “Survey on Wheel Slip Control Design Strategies Evaluation and Application to Antilock Braking Systems,” *IEEE Access*, vol. 8, pp. 10951-10970, 2021. doi: 10.1109/ACCESS.2020.2965644

(4) M. Tanelli, A. Astolfi, and S.M. Savaresi, “Robust nonlinear proportional-integral control for active braking control systems,” *Proceedings of the IEEE Conference on Decision and Control*, pp. 1745-1750, San Diego, U.S., Dec. 13-15, 2006.

(5) D. Savitski et al., ”Robust continuous wheel slip control with reference adaptation: Application to the brake system with decoupled architecture,” *IEEE Transactions on Industrial Informatics*, vol. 14(9), pp. 4212-4223, 2018. doi: 10.1109/TII.2018.2817588

(6) F. Pretagostini, B. Shyrokau, and G. Berardo, “Anti-lock braking control design using a nonlinear model predictive approach and wheel information,” *Proceedings of the IEEE International Conference on Mechatronics*, pp. 525-530, Ilmenau, Germany, March 18-20, 2019. doi: 10.1109/ICMECH.2019.8722841

(7) D. Tavernini et al., “An explicit nonlinear model predictive ABS controller for electro-hydraulic braking systems,” *IEEE Transactions on Industrial Electronics,* vol. 67(5), pp. 3990-4001, 2019. doi: 10.1109/TIE.2019.2916387

(8) P. Khatun et al., “Application of fuzzy control algorithms for electric vehicle antilock braking/traction control systems", *IEEE Transactions on Vehicular Technologies*, vol. 52(5), pp. 1356-1364, 2013. doi: 10.1109/TVT.2003.815922

(9) A. Aksjonov et al., “Hardware-in-the-Loop Test of an Open Loop Fuzzy Control Method for Decoupled Electro-Hydraulic Antilock Braking System,” *IEEE Transactions on Fuzzy Systems*, vol. 29(5), pp. 965-975, 2020. doi: 10.1109/TFUZZ.2020.2965868

(10) J. Guo, X. Jian, and G. Lin, “Performance evaluation of an anti-lock braking system for electric vehicle with fuzzy sliding mode controller,” *Energies*, vol. 7(10), pp. 6459-6476, 2014. doi: 10.3390/en7106459

(11) H.-Z. Li et al., “PID plus fuzzy logic method for torque control in traction control system,” *Int. J. Autom. Technol.*, vol. 13(3), pp. 441-450, 2012. doi: 10.1007/s12239-012-0041-4

(12) C.-M. Lin, and H.-Y. Li, “Intelligent hybrid control system design for antilock braking systems using self-organizing function-link fuzzy cerebellar model articulation controller,” *IEEE Transactions on Fuzzy Systems*, vol. 21(6), pp. 1044-1055, 2013. doi: 10.1109/TFUZZ.2013.2241769

(13) O. Cerman and P. Hušek, “Adaptive fuzzy sliding mode control for electro-hydraulic servo mechanism,” *Expert System Applications*, vol. 39(1), pp. 10269-10277, 2012. doi: 10.1016/j.eswa.2012.02.172

(14) S. L. Peric et al., “Quasi-sliding mode control with orthogonal endocrine neural network-based estimator applied in anti-lock braking system,” *IEEE/ASME Trans. Mechatronics*, vol. 21(2), pp. 754-764, 2016. doi: 10.1109/TMECH.2015.2492682

(15) Deutsches Institut für Normung e. V. (DIN), ”Hydraulic braking systems; dual circuit brake systems; symbols for brake circuits diagrams”, DIN 74000, August 1992.

(16) International Organization for Standardization (ISO), “Road vehicles – Functional Safety”, ISO 26262, December 2018.

(17) M. Heydrich et al., “Hardware-in-the-Loop Testing of a Hybrid Brake-by-Wire System for Electric Vehicles”, *SAE Int. J. Veh. Dyn., Stab., and NVH*, vol. 6(4), pp. 477-487, 2022. doi: 10.4271/10-06-04-0031

(18) M. Heydrich et al., “Integrated Braking Control for Electric Vehicles with In-Wheel 2 Propulsion and Fully Decoupled Brake-by-Wire System,” *Vehicles*, vol. 3(2), pp. 145-161, 2021. doi: 10.3390/vehicles3020009

(19) Economic Commission for Europe, “ECE-R13H: Uniform Provision concerning the approval of vehicles of categories M, N and O with regard to braking,” December 2015.

(20) H. W. Kummer, “Unified Theory of Rubber and Tire Friction,” *Engineering Research Bulletin B-94*, Pennsylvania State University, pp. 100 – 101, 1966.

(21) H. Zhang, Z. Zhang, and J. Liang, “Dynamic driving intention recognition of vehicles with different driving styles of surrounding vehicles,” *IET Intelligent Transport Systems*, vol. 16(9), pp. 571-585, 2021. doi: 10.1049/itr2.12158

APPENDIX

Table 2 Final control gains of the continuous approaches

	PI			ISM
	K_p	t_i	t_a	K_{ism}
Front axle	25000	1.6	1.2	100
Rear axle	36000	0.85	0.6	700

Table 3 Percentual improvement of KPIs for all manoeuvers on high μ surface

v_{init}	s_{br}		d_m		TE (FL)		TE (RR)		IACA	
[km/h]	ISM	PI	ISM	PI	ISM	PI	ISM	PI	ISM	PI
50	4.51	4.75	9.53	9.73	23.26	24.08	6.29	6.62	-5,56	-5,84
70	5.62	5.78	11.19	11.38	12.14	8.01	0.67	2.99	-7,53	-7,67
100	2.55	2.47	4.89	4.69	8.39	8.16	0.34	-0.23	-4,02	-3,92
130	2.85	2.60	4.84	5.10	6.78	9.67	2.84	-0.06	-4,53	-4,41
160	3.87	3.94	6.14	6.23	5.96	5.76	5.14	9.71	-5,97	-6,06

Table 4 Percentual improvement of KPIs for all manoeuvers on low μ surface

v_{init}	s_{br}		d_m		TE (FL)		TE (RR)		IACA	
[km/h]	ISM	PI	ISM	PI	ISM	PI	ISM	PI	ISM	PI
50	3,31	2.91	11.69	10.72	47,84	48,21	42,59	59,99	30,50	30,20
70	9,73	9.33	20.26	19.67	52,05	46,65	59,48	45,18	25,74	23,29
100	9,57	9.48	18.32	18.30	58,73	58,13	71,95	70,18	28,94	28,88
130	13,56	13.76	25.78	26.36	56,07	54,02	44,38	66,28	24,03	23,55
160	10,74	9.91	18.65	16.33	52,93	50,51	68,02	69,85	24,04	23,03

Table 5 Percentual improvement of KPIs for all manoeuvers on split μ surface

v_{init}	s_{br}		d_m		TE (FL)		TE (RR)		IACA	
[km/h]	ISM	PI	ISM	PI	ISM	PI	ISM	PI	ISM	PI
50	9,59	9,37	19,94	19,79	7,05	6,52	4,48	-0,45	-1,41	-1,27
70	9,49	9,76	18,23	18,95	12,73	7,70	-23,76	-24,29	-3,63	-4,82
100	6,11	2,02	5,90	-2,64	26,88	27,37	-20,64	2,61	-0,55	5,17
130	5,37	8,18	3,41	10,19	32,21	32,03	4,25	22,29	-3,12	-6,79
160	3,40	5,86	1,34	5,56	32,82	32,22	-19,20	13,01	-3,21	-5,94

Table 6 Percentual improvement of KPIs for all manoeuvers on longitudinal split μ surface

v_{init}	s_{br}		d_m		TE (FL)		TE (RR)		IACA	
[km/h]	ISM	PI	ISM	PI	ISM	PI	ISM	PI	ISM	PI
50	3,00	3,76	5,35	6,51	10,75	7,08	29,69	29,18	-8,98	-4,05
70	6,81	6,53	10,75	10,29	46,36	44,30	52,28	59,75	-20,56	-18,00
100	7,23	7,93	12,21	13,46	47,94	43,23	48,78	51,60	-12,01	-10,86
130	8,84	8,58	13,13	12,83	56,46	60,03	51,56	52,32	-20,66	-21,68
160	8,77	9,75	13,25	14,73	49,82	48,81	44,09	46,30	-18,63	-16,56

Table 7 Percentual improvement of KPIs for all manoeuvers on patch μ surface

v_{init}	s_{br}		d_m		TE (FL)		TE (RR)		IACA	
[km/h]	ISM	PI	ISM	PI	ISM	PI	ISM	PI	ISM	PI
50	1,65	1,76	3,04	3,18	27,03	25,03	43,06	43,53	1,19	1,03
70	-1,36	-0,69	0,12	1,33	4,46	3,34	63,37	61,18	-0,13	-0,41
100	3,42	3,37	5,30	5,25	6,63	13,00	39,14	40,30	-4,11	-3,81
130	0,30	-0,36	0,44	0,00	1,03	0,92	0,60	29,59	-1,13	-0,45
160	1,60	1,00	1,25	0,38	-0,98	1,00	-28,64	-3,74	-2,79	-2,15